World Academy of Science, Engineering and Technology
International Journal of Computer and Information Engineering
Vol:11, No:7, 2017

# An Improved Sub-Nyquist Sampling Jamming Method for Deceiving Inverse Synthetic Aperture Radar

Yanli Qi, Ning Lv, Jing Li



***Abstract*—**Sub-Nyquist sampling jamming method (SNSJ) is a well known deception jamming method for inverse synthetic aperture radar (ISAR). However, the anti-decoy of the SNSJ method performs easier since the amplitude of the false-target images are weaker than the real-target image; the false-target images always lag behind the real-target image, and all targets are located in the same cross-range. In order to overcome the drawbacks mentioned above, a simple modulation based on SNSJ (M-SNSJ) is presented in this paper. The method first uses amplitude modulation factor to make the amplitude of the false-target images consistent with the real-target image, then uses the down-range modulation factor and cross-range modulation factor to make the false-target images move freely in down-range and cross-range, respectively, thus the capacity of deception is improved. Finally, the simulation results on the six available combinations of three modulation factors are given to illustrate our conclusion.

***Keywords*—**Inverse synthetic aperture radar, ISAR, deceptive jamming, Sub-Nyquist sampling jamming method, SNSJ, modulation based on Sub-Nyquist sampling jamming method, M-SNSJ.

## I. Introduction

ISAR plays a remarkable role in military applications for all-weather, day-night and high-resolution capability [1]-[4]. ISAR jamming and anti-jamming have become a hotspot in current research; since blanketing jamming consumes more power, more studies on deception jamming have been performed.

In recent years, a variety of ISAR deception methods have been proposed. In [5], digital false-target image synthesizer (DIS) is presented to create false targets. In [6], [7], authors propose some improvements to decrease the computational complexity and realize multi-false-targets deception. However, the method still presents high complexity according to the jamming principle. A practical method of multiplication jamming in [8] is proved to be feasible. However, it is difficult to keep consistent between the false-target images and the real-target image since the changing of ISAR image templates depends on the ISAR incident angle which is difficult to attain. It is noted above that both DIS and multiplication jamming need accurate parameters obtained by detective work. In order to simplify the jamming process, Digital Radio Frequency Memory (DRFM) is introduced to generate ISAR echoes in [9]. In [10], [11], SNSJ method is proposed. This algorithm does not require any computation, only need high quality analogue-to-digital converter (ADC). The jamming echoes are also reflected from the target, which guarantee the consistency of the false-target images and real-target image. In summary, SNSJ turns out to be effective and can be realized easily. However, problems still exist in SNSJ. At first, if the jammer transmits intercepted signals directly, the intensity of the false-target images will be weaker than the real-target image. So the power of the intercepted signals needs to be magnified appropriately. Secondly, the jamming echoes are always behind the ISAR echoes from the target, so the false-target images are behind the real-target image, too. In order to solve the problem, we propose an improved method in this paper to compensate the signal delay by multiplying a down-range modulation factor. In this way, the false-target images' position will be free in down-range. Similarly, the false-target images in [7], [8] only appear in the same cross-range, we expand the range of the false-target images by multiplying the cross-range modulation factor.

Yanli Qi is with Xidian University, Xi'an, 710071 China (corresponding author, phone: +86 18710847090; e-mail: 690348510@qq.com).
Ning Lv and Jing Li are with Xidian University, Xi'an, 710071 China (e-mail: nlv@mail.xidian.edu.cn, 1395380078@qq.com).

## II. Formulation of M-SNSJ

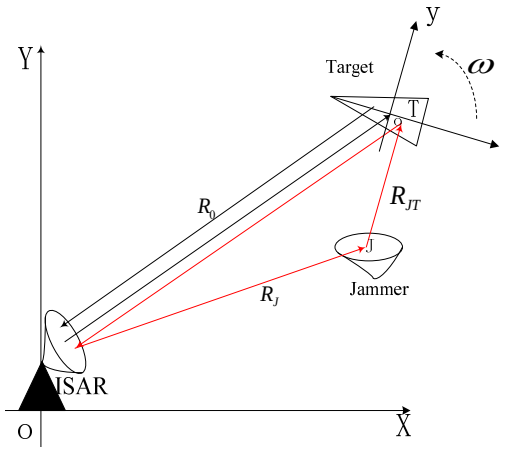


Fig. 1 ISAR imaging model of SNSJ

For brevity, we analyze and solve problems in two dimensions in this paper. As shown in Fig. 1, ISAR is located at the point designated as $O$, the target is located at T, and the jammer is located at J. The distance between ISAR and jammer, ISAR and target, jammer and target are $R_J$, $R_0$, $R_{JT}$ respectively. The ISAR is in XOY coordinate system, and the two dimensional coordinate xoy is embedded on the target whose center is the origin o. The rigid-body target circular

motion is described as $\theta_i(t)=\theta_{i0}+\omega t$ with the rotation rate $\omega$ (rad/s) and initial angle $\theta_{i0}$ (rad).

Since ISAR transmits a linear frequency modulated (LFM) pulse with the center frequency designated as $f_0$ and the chirp rate designated as $k$, the waveform of the transmitted signal in fast-time domain and slow-time domain can be expressed as (1):

$$\begin{aligned} s(\hat{t},t_m) &= rect(\hat{t}/T_p)\exp(j\pi k\hat{t}^2)\exp[j2\pi f_0(\hat{t}+t_m)] \\ &= \mu(\hat{t})\exp[j2\pi f_0(\hat{t}+t_m)]. \end{aligned} \tag{1}$$

where $\mu(\hat{t})=rect(\hat{t}/T_p)\exp(j\pi k\hat{t}^2)$, $\hat{t}$ is the fast time, $t_m$ is the slow time, and $T_p$ is the pulse width which yields 1 when $(\hat{t}/T_p)\le 0.5$, otherwise yields 0.

Assuming that the intermittent sampling signal in jammer is:

$$p(t)=rect(t/\tau)\sum_{n=-\infty}^{+\infty}\delta(t-nT_s). \tag{2}$$

where $\tau$ is the pulse width, $T_s$ is the sampling period, $\delta(\bullet)$ is the impact function, respectively. The working time sequence of the jammer is illustrated in Fig. 2.

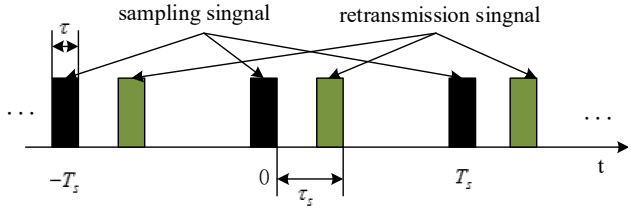


Fig. 2 Sampling and retransmission by jammer

As shown in Fig. 1, if the echoes are reflected from the target directly, the time delay is $\tau_0=2R_0/c$. According to (1), the echoes will be expressed as (3):

$$\begin{aligned} s_0(\hat{t}-\tau_0,t_m) &= rect((\hat{t}-\tau_0)/T_p)\exp(j\pi k(\hat{t}-\tau_0)^2) \\ &\quad\cdot\exp[j2\pi f_0(\hat{t}-\tau_0+t_m)] \\ &= \mu((\hat{t}-\tau_0))\exp[j2\pi f_0((\hat{t}-\tau_0)+t_m)]. \end{aligned} \tag{3}$$

When the jammer starts to work, the jamming echoes will be reflected from the target in a zigzag way. The time delay is $\tau_J=(R_0+R_J+R_{JT})/c+\tau_s$, where $\tau_s$ is the time delay between sampling and retransmission, which is controlled by the jammer. The jamming echoes will be expressed as (4):

$$\begin{aligned} s_J(\hat{t},t_m) &= p(t)s(\hat{t}-\tau_J,t_m) \\ &= \left(rect(t/\tau)\sum_{n=-\infty}^{+\infty}\delta(t-nT_s)\right)rect((\hat{t}-\tau_J)/T_p) \\ &\quad\cdot\exp(j\pi k(\hat{t}-\tau_J)^2)\exp[j2\pi f_0(\hat{t}-\tau_J+t_m)] \\ &= \left(rect(t/\tau)\sum_{n=0}^{N-1}\delta(t-\tau_J-nT_s)\right) \\ &\quad\cdot\exp[j\pi k(\hat{t}-\tau_J)^2]\exp[j2\pi f_0((\hat{t}-\tau_J)+t_m)]. \end{aligned} \tag{4}$$

where $N=|T_P/T_s|$, $|\bullet|$ demonstrate ceil operation. When the echoes are received, the dechirping operation will be done later. Suppose that the reference distance is $R_{ref}$, the reference time is $t_{ref}$, the dechirping result can be written as (5):

$$\begin{aligned} \overline{s}_J(\hat{t},t_m) &= s_J(\hat{t},t_m)conj[s(\hat{t}-t_{ref},t_m)] \\ &= \left(rect(t/\tau)\sum_{n=0}^{N-1}\delta(t-\tau_J-nT_s)\right) \\ &\quad\cdot\exp[j2\pi k(t_{ref}-\tau_J)\hat{t}]\exp[j2\pi f_0(t_{ref}-\tau_J+t_m)]. \end{aligned} \tag{5}$$

Then, after range compression, the result can be expressed as (6):

$$\begin{aligned} \overline{s}_J(f_r,t_m) &= \left(rect(t/\tau)\sum_{n=0}^{N-1}\delta(t-\tau_J-nT_s)\right) \\ &\quad\cdot\exp[j2\pi k(t_{ref}-\tau_J)\hat{t}]\exp[j2\pi f_0(t_{ref}-\tau_J+t_m)] \\ &= \sum_{n=-\infty}^{+\infty}\tau f_s T_p\sin c(nf_s\tau)\sin c(T_p(f_r-nf_s-k(\tau_J-t_{ref}))) \\ &\quad\cdot\exp[j2\pi f_0(t_{ref}-\tau_J+t_m)]. \end{aligned} \tag{6}$$

where $\sin c(x)=\sin(\pi x)/\pi x$. By using the conversion relationship between time domain and frequency domain, (6) can be converted into the expression as (7):

$$\begin{aligned} \overline{s}_J(r,t_m) &= \sum_{n=-\infty}^{+\infty}DT_p\sin c(nD)\exp[-j2\pi f_0(t_{ref}-\tau_J+t_m)] \\ &\quad\cdot\sin c(2B/c(r-ncf_s/2k-c(\tau_J-t_{ref})/2)). \end{aligned} \tag{7}$$

where $D=\tau f_s=\tau/T_s$ is the duty ratio of intermittent sampling signal. $\tau_J-t_{ref}$ changes with the azimuth echoes. If $\tau_J-t_{ref}$ changes violently, range alignment should be performed. Then the Fourier transform can be done in the cross-range, the two dimension image in ISAR will be obtained as (8):

$$\begin{aligned} &\overline{s}_J(r,f)= \\ &\sum_{i=1}^{I}\left\{\begin{array}{l}\sum_{n=-\infty}^{+\infty}DT_pT_M\sin c(nD)\sin c(2B/c(r-ncf_s/2k-ct_r/2)) \\ \cdot\sin c(T_M(f-2f_0\omega/cX_i))\exp(-j2\pi(R_{total}-R_{ref})/c)\end{array}\right\}. \end{aligned} \tag{8}$$

where $T_M$ is the accumulation time in the cross-range, $R_{total} = R_J + R_{JT} + R_0 + 2\Delta R_i$ is the route length of the jamming signal, $I$ is the total scattering. From (8), It can be seen that the intermittent sampling signal will lead to a series of false-target images in down-range.

## III. Proposed Method

In order to get more effective false-target images in ISAR, we will present improved modulations from the following three aspects. The schematic diagram of the proposed method is illustrated in Fig. 3.

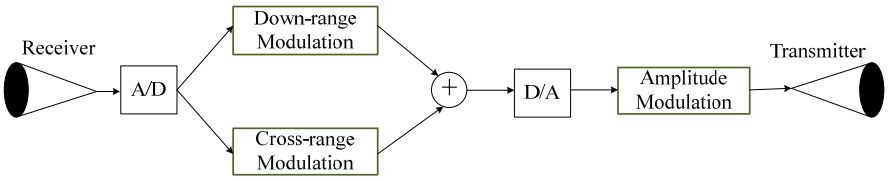


Fig. 3 The schematic diagram of M-SNSJ

### A. Power Modulation

The power of target echoes can be derived from the radar equation as (9):

$$P_r = \frac{P_t G^2 \lambda^2 \sigma}{(4\pi)^3 R_0^4}. \quad (9)$$

Also, the power of jamming echoes can also be calculated by radar equation. It can be represented as (10):

$$\bar{P}_r = \frac{P_t G^2 \lambda^2 \sigma D}{(4\pi)^3 R_0^2 (R_J + R_{JT})^2}. \quad (10)$$

Considering that the SNSJ could get multiple false-target images, and the amplitude of each false-target image is different, which can be concluded from (8). The amplitude of the nth false-target image is $DT_p T_M \sin c(nD)$. In order to get the average amplitude of each false-target image, the number of the false-target images has to be obtained. Suppose that the target takes up $D_r$ units in down-range, normally, the distance between two adjacent false-target images should be greater than $D_r$. The distance between two adjacent false-target images in down-range is $cf_s/2k$ which can be concluded from (8), so $D_r$ should satisfy (11):

$$cf_s/2k \geq D_r. \quad (11)$$

considering the limit case, when $cf_s/2k = D_r$, the maximum number of false-target images will be:

$$N_{\max} = D_d / D_r. \quad (12)$$

where $D_d$ is the total length of down-range. Typically, the number of false-target images is $N = 2kD_d / cf_s$, so the power of each false target is:

$$\bar{P}_{r\_1} = \bar{P} / N = \frac{P_t G^2 \lambda^2 \sigma D cf_s}{(4\pi)^3 R_0^2 (R_J + R_{JT})^2 2kD_d}. \quad (13)$$

In order to get the most effective jamming result, $P_r$ and $\bar{P}_{r\_1}$ should satisfy (14):

$$P_r = \frac{P_t G^2 \lambda^2 \sigma}{(4\pi)^3 R_0^4} \leq \bar{P}_{r\_1} = \frac{P_t G^2 \lambda^2 \sigma D cf_s}{(4\pi)^3 R_0^2 (R_J + R_{JT})^2 2kD_d}. \quad (14)$$

We can get (15) derived from (14):

$$R_0^2 \geq (R_J + R_{JT})^2 2kD_d / cf_s D. \quad (15)$$

Typically, the (15) is difficult to satisfy. So a power amplifier is used in the power modulation module of a jammer. According to above analysis, modulation factor which is designated as $F_a$ should satisfy (16):

$$F_a = R_0^2 cf_s / \left[ (R_J + R_{JT})^2 2k \right]. \quad (16)$$

Certainly, if the modulation factor is large enough

$$F_a \gg R_0^2 cf_s / \left[ (R_J + R_{JT})^2 2k \right]. \quad (17)$$

the false-target images will make the real-target image invisible.

### B. Down-Range Modulation

As shown in Fig. 2, the time delay of the target echoes is:

$$\tau_0 = 2R_0 / c. \quad (18)$$

The time delay of the jamming echoes is

$$\tau_J = (R_0 + R_J + R_{JT}) / c. \quad (19)$$

As $R_0$, $R_J$ and $R_{JT}$ formed a triangle. With the nature relationship between sides of the triangle $R_J + R_{JT} > R_0$, we have $\tau_J > \tau_0$. Therefore, the jamming echoes will lag behind the target echoes, which makes anti-interference easier. In

order to solve this problem, we propose the down-range modulation factor based on the theory of time-frequency relation to amend the jamming echo. It can be represented as:

$$s_{\Delta J}\left(\hat{t}+\Delta\tau,t_m\right)=s_J\left(\hat{t},t_m\right)F_{d\_t}\,. \tag{20}$$

$$\begin{aligned}
s_J\left(\hat{t}+\Delta\tau,t_m\right)&=p(t)s\left(\hat{t}-\tau_J+\Delta\tau,t_m\right)\\
&=\left(rect(t/\tau)\sum_{n=-\infty}^{+\infty}\delta\left(t-nT_s\right)\right)rect\left(\left(\hat{t}-\tau_J+\Delta\tau\right)/T_p\right)\\
&\cdot\exp\left(j\pi k\left(\hat{t}-\tau_J+\Delta\tau\right)^2\right)\exp\left[j2\pi f_0\left(\hat{t}-\tau_J+\Delta\tau+t_m\right)\right]\\
&=\left(rect(t/\tau)\sum_{n=0}^{N-1}\delta\left(t-\tau_J-nT_s\right)\right)\exp\left[j\pi k\left(\hat{t}-\tau_J+\Delta\tau\right)^2\right]\\
&\cdot\exp\left[j2\pi f_0\left(\left(\hat{t}-\tau_J+\Delta\tau\right)+t_m\right)\right]\\
&=s_J\left(\hat{t},t_m\right)\exp\left[j\pi k\left(\Delta\tau^2+2\Delta\tau(\hat{t}-\tau_J)\right)\right]\exp\left[j2\pi f_0\Delta\tau\right]\\
&=s_J\left(\hat{t},t_m\right)F_{d_t}\,.
\end{aligned} \tag{21}$$

where $s_J\left(\hat{t}+\Delta\tau,t_m\right)$ is the signal after down-range modulation in time domain. $F_{d\_t}$ is the down-range modulation factor in time domain.

### C. Cross-Range Modulation

As shown in (8), all the false-target images will be located at the same cross-range. In order to get a better deception, we propose to expand the cross-range of the false-target images by using the cross-range modulation module in jammer. Similarly, considering the principle of ISAR imaging in cross-range, such as the classical algorithm range-Doppler algorithm (RD) in ISAR imaging; if we want to shift the image in cross-range, we need to add an extra static frequency satisfying (22):

$$s_{\Delta J}\left(\hat{t},f-f_c\right)=s_J\left(\hat{t},f\right)F_{c\_f}\,. \tag{22}$$

where $s_{\Delta J}\left(\hat{t},f-f_c\right)$ is the signal after cross-range modulation in frequency domain. $f_c$ is the frequency shift, which can be positive or negative. $F_{c\_f}$ is the cross-range modulation factor in frequency domain. Using the well-known Fourier transform and taking into account the major influence in cross-range. Equation (22) can be represented as:

$$\begin{aligned}
s_{\Delta J}\left(\hat{t},t_m\right)&=s_J\left(\hat{t},t_m\right)F_{c_t}\approx s_J\left(\hat{t},t_m\right)\exp(j2\pi f_c t_m)\\
F_{c_t}&\approx\exp(j2\pi f_c t_m)\,.
\end{aligned} \tag{23}$$

where $s_{\Delta J}\left(\hat{t},t_m\right)$ is the signal after cross-range modulation in time domain. $F_{c\_t}$ is the cross-range modulation factor in time domain. Since the original false-target images should be displayed in ISAR, we make the received radar signal go through a 2-way power splitter. Then we use two power amplifiers on each path. Finally an adder is used to composite signal. Fig. 4 shows the cross-range modulation workflow of the jammer.

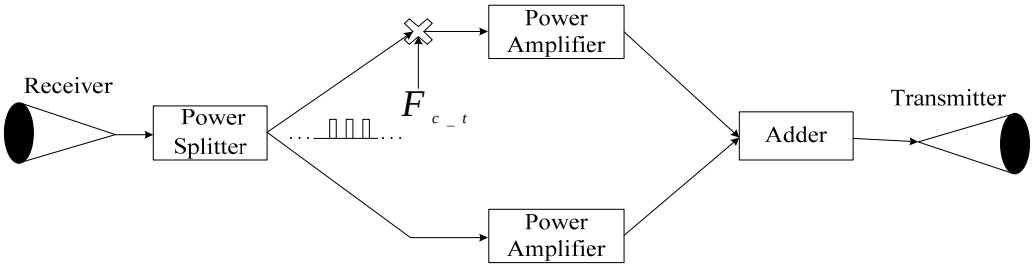


Fig. 4 The cross-range modulation workflow of the jammer

## IV. Simulation Results

The supposed range-Doppler ISAR imaging scenario is illustrated in Fig. 1. The target, radar and jammer parameters with respect to the scenario are listed in Table I. The target is assumed to be composed of a number of perfect points scattering evenly on the radar cross section (RCS). Their locations in the 2D coordinate system are plotted in Fig. 5.

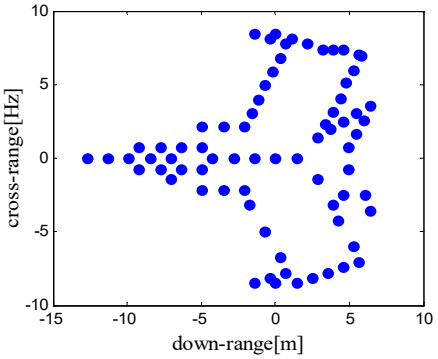


Fig. 5 Aircraft scattering point model

TABLE I
TARGET, RADAR AND JAMMER PARAMETERS

| Symbol | Parameter name | Value |
|---|---|---|
| $N_s$ | scatter number | 34 |
| $\omega$ | angular velocity | 0.01 rad/s |
| $f_0$ | center frequency | 10 GHz |
| $B$ | frequency bandwidth | 200 MHz |
| $f_s$ | sampling frequency of ISAR | 480 MHz |
| $T_p$ | pulse width | 10 us |
| $PRF$ | pulse repetition frequency | 500 Hz |
| $R_0$ | distance between target and ISAR | 5 Km |
| $R_J$ | distance between target and jammer | 25 m |
| $R_{JT}$ | distance between jammer and ISAR | 5 Km |
| $T_s$ | sampling period of jammer | 0.02 us |
| $D$ | duty ratio of jammer | 50% |

### A. Experiment 1: Comparison of SNSJ and M-SNSJ

1) Power Modulation Simulation

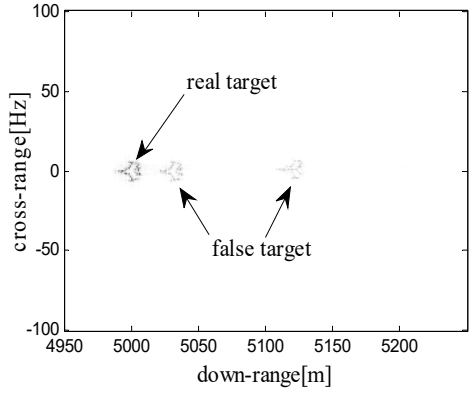


(a) The ISAR image before power modulation

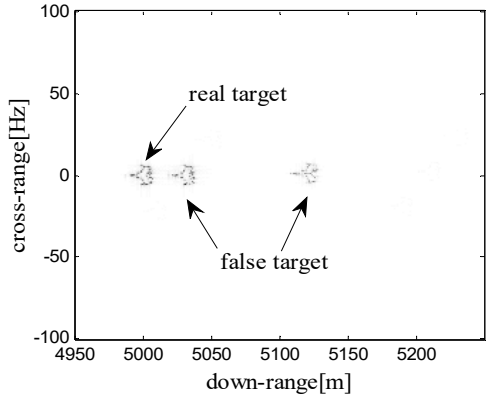


(b)The ISAR image after power modulation

Fig. 6 The simulation results on power modulation

The distance between the false targets is $cf_s/2B \approx 90m$, the ISAR image size is 250 m, and thus, there are two false targets in the image. And the gain of power amplifier is 3dB. In Fig. 6 (a), it is obvious that the false targets are weaker than the real target before power modulation. The power modulation simulation result is shown in Fig. 6 (b). It shows that the false targets and the real target have the same intensity, which enhances the deceptive effect of the false targets.

2) Down-Range Modulation Simulation

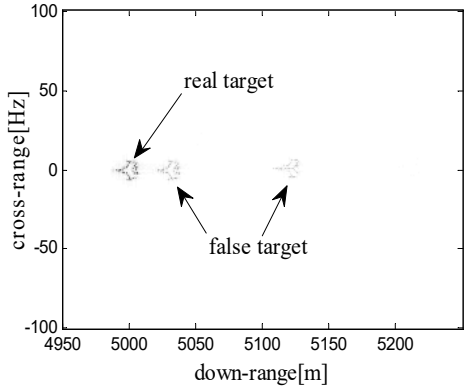


(a) The ISAR image before down-range modulation

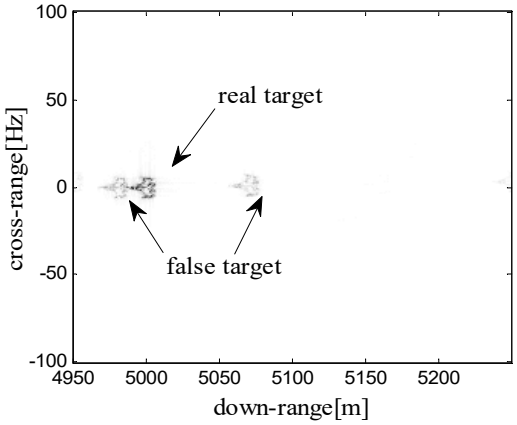


(b) The ISAR image after down-range modulation

Fig. 7 The simulation results on down-range modulation

The down-range modulation factor in down range is 50m, the modulation result image illustrated in Fig. 7 (b) shows that the false target has moved forward 50m, which is consistent with settings. This operation largely avoids the real target being attacked at first.

3) Cross-Range Modulation Simulation

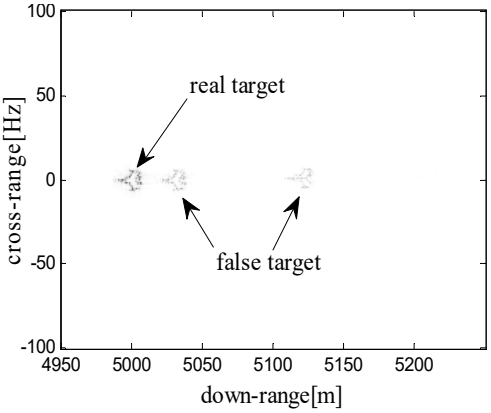


(a) The ISAR image before cross-range modulation

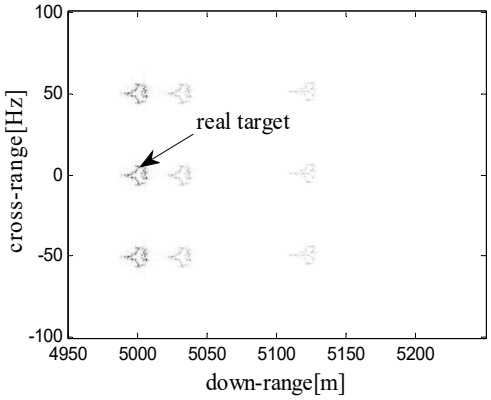


(b) The ISAR image after cross-range modulation.

Fig. 8 The simulation results on cross-range modulation

The cross-range modulation factors in the cross-range are 50Hz and -50Hz, the modulation results image illustrated in Fig. 8 (b) shows that the target moves up and down 50Hz. Multiple false targets appear in the scene, so it is more difficult for enemies to identify the real target.

### *B. Experiment 2: Different Combinations of Modulation*

Since these modulation factors are independent, they can be combined freely. Fig. 9 shows the simulation result of different combination modes. Fig. 9 (a) is the ISAR image without modulation, in which it is easy to find out the real target. Fig. 9 (b) is the ISAR image with power and down-range modulation. The false target and the real target have the same power, the false targets appear in front of the real targets, so the false targets protect the real targets from being found effectively. Fig. 9 (c) is the ISAR image with power and cross-range modulation. Multiple false targets appear on both sides of the real target, and the number of the false targets increased several times. Fig. 9 (d) is the ISAR image with power, down-range and cross-range modulation. The real target is wrapped up in the middle of eight false targets, which may be the best approach to protect the real target. To sum up, we can use different modulation combinations to get different deceptive effects.

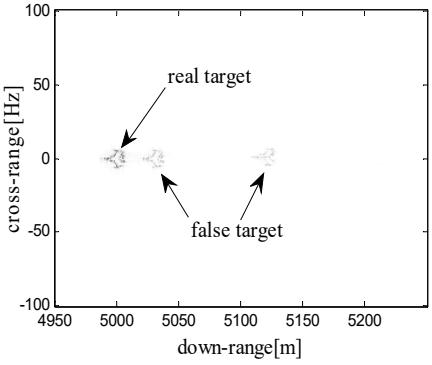


(a) The ISAR image without modulation

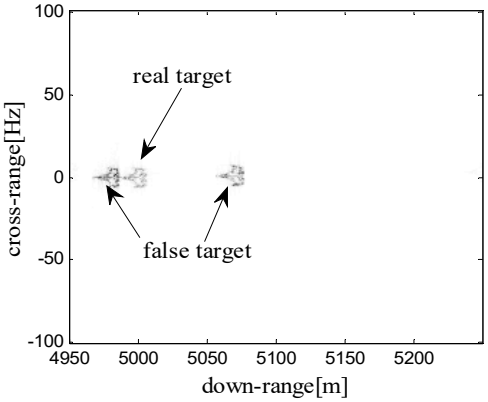


(b) The ISAR image with power and down-range modulation

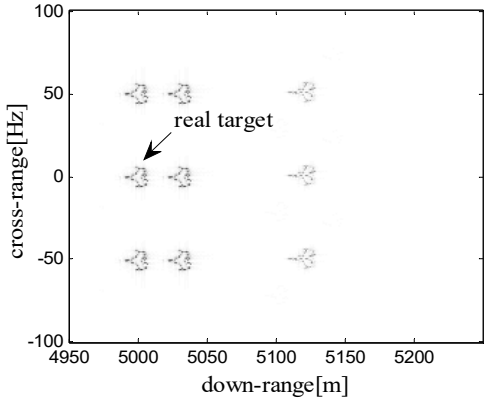


(c) The ISAR image with power and cross-range modulation

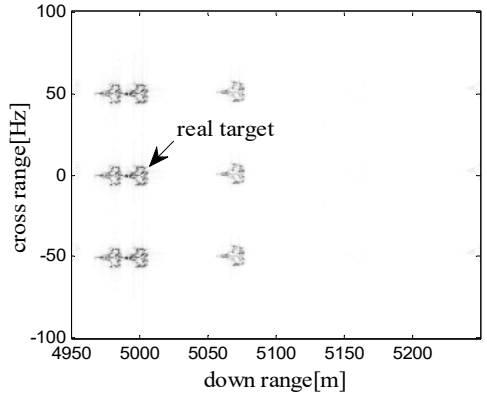


(d) The ISAR image with power, down-range and cross-range modulation

Fig. 9 The ISAR image of different combinations of modulation mode

## V. Conclusion

In conclusion, an Improved Sub-Nyquist Sampling Jamming Method (M-SNSJ) is proposed to overcome the shortcomings of the SNSJ and successfully verified by the simulation. The proposed scheme consists of three parts, namely power modulation, down-range modulation and cross-range modulation. The power modulation is to make it hard to identify the true target by adjusting the power of the false targets to the level of the real target. The down-range

modulation makes the false targets appear in any position in down-range. Similarly, the cross-range modulation makes the target appear in any cross-range to enhance the flexibility of the deception. More importantly, the three modulations can be used in combination freely. The simulation results show that the deceptive effect of M-SNSJ is better than SNSJ.

## REFERENCES

[1] T. Wang, X. Wang, Y. Chang, J. Liu, and S. Xiao, "Estimation of precession parameters and generation of ISAR images of ballistic missile targets," *IEEE Trans. Aerosp. Electron. Syst.*, vol. 46, no. 4, pp. 1983–1995, Oct. 2010.

[2] Xueru Bai, "Study on New Techniques for ISAR Imaging of Aerospace Targets" (D), 2011.

[3] M. Skolnik, *Radar Handbook*, 3rd ed. New York, NY, USA: McGraw Hill, 2008.

[4] X.-C. Xie and Y.-H. Zhang, "High-resolution imaging of moving train by ground-based radar with compressive sensing," *Electron. Lett.* vol. 46, no. 7, pp. 529–531, Apr. 2010.

[5] P. E. Pace, D. J. Fouts, S. Ekestorm, and C. Karow, "Digital false-target image synthesiser for countering ISAR," *IEE Proc. Radar Sonar Navig*. vol. 149, no. 5, pp. 248–257, Oct. 2002.

[6] Letao Xu, Dejun Feng, Xiaoyi Pan, Qingfu Liu, and Xuesong Wang, "An Improved Digital False-Target Image Synthesizer Method for Countering Inverse Synthetic Aperture Radar", *IEEE Sensors J*, vol. 15, no. 10, Oct 2015.

[7] Li Yuan, Lv Gaohuan, Chen Huilian, "The Study of Multi-false Targets Deception against Stepped-frequency Waveform Inverse Synthetic Aperture Radar", *ICSP2008 Proceedings*.

[8] Xu, Letao, Fend Dejun, Liu QINGFU, et al ISAR Decoy Generation by Utilizing Coherent Multiplication Method Jamming, *Acta Electronica Sinica*, Vol.42 No 12. Dec 2014.

[9] Wang Chao, Zhang Xiao-fa and Yuan Nai-chang: *Journal of system Simulation* 19 (2007) 4639.

[10] X. Pan, W. Wang, D. Feng, Y. Liu, Q. Fu, and G. Wang, "On deception jamming for countering bistatic ISAR based on sub-nyquist sampling," *IET Radar, Sonar Navigat.*, vol. 8, no. 3, pp. 173–179, Mar. 2014.

[11] W. Wang, X.-Y. Pan, Y. C. Liu, D.-J. Feng, and Q.-X. Fu, "Sub-Nyquist sampling jamming against ISAR with compressive sensing," *IEEE Sensors J*, vol. 14, no. 9, pp. 3131–3136, Sep. 2014.